Journal of Organometallic Chemistry, *445* (1993) 187–198

JOM 23155

Cluster chemistry

LXXXIII *. Reactions of $Ru_5(\mu_5\text{-}C_2PPh_2)(\mu\text{-}PPh_2)(CO)_{13}$ with olefins: Products formed by addition of an alkene to the C_2 fragment. X-ray structures of $Ru_5(\mu_4\text{-}PPh)\{\mu_4\text{-}C_2(CHCHR)CHCH_2R\}(\mu\text{-}PPh_2)\text{-}(CO)_{12}$ (R = H, Me) and $Ru_5(\mu_4\text{-}PPh)(\mu\text{-}PPh_2)(\mu\text{-}CO)(CO)_{10}\text{-}\{\eta^5\text{-}C_5H_3Me\text{-}1\text{-}(CH{=}CH_2)\text{-}3\}$

Chris J. Adams, Michael I. Bruce, Michael J. Liddell and Edward R.T. Tiekink
Jordan Laboratories, Department of Physical and Inorganic Chemistry, University of Adelaide, Adelaide, S.A. 5001 (Australia)

Brian W. Skelton and Allan H. White
Department of Chemistry, University of Western Australia, Nedlands, W.A. 6009 (Australia)

(Received August 5, 1992)

Abstract

Addition of two molecules of ethene to the C_2PPh_2 unit of $Ru_5(\mu_5\text{-}C_2PPh_2)(\mu\text{-}PPh_2)(CO)_{13}$ (**1**) produced two isomers of $Ru_5(\mu_4\text{-}PPh)\{\mu_4\text{-}C_2(CHCH_2)CHMe\}(\mu\text{-}PPh_2)(CO)_{12}$ (**4a**, **4b**). The metal core consists of a wing-tip-bridged butterfly, one Ru_4 face of which is capped by a carbon atom of a hydrocarbon ligand formed by addition of two molecules of ethene to one carbon of a C_2 unit derived from the C_2PPh_2 ligand. The other Ru_4 face is capped by a μ_4-PPh group. The isomers differ in the relative locations of the μ-PPh_2 and CO groups. Reactions with propene and but-1-ene yielded the analogous complexes $Ru_5(\mu_4\text{-}PPh)(\mu_4\text{-}C_2(CHCHR)CHCH_2R)(\mu\text{-}PPh_2)(CO)_{12}$ [R = Me (**5a**, **5b**), Et (**6a**, **6b**)]. Reaction of **4a** with further ethene produced $Ru_5(\mu_4\text{-}PPh)(\mu\text{-}PPh_2)(\mu\text{-}CO)(CO)_{10}\{\eta^5\text{-}C_5H_3Me\text{-}1\text{-}(CH{=}CH_2)\text{-}3\}$ (**8**), in which a square pyramidal Ru_5 core is capped on the square face by a μ_4-PPh ligand. One basal edge is bridged by the μ-PPh_2 group and one of the other basal Ru atoms carries the disubstituted cyclopentadienyl ligand, which has been formed by combination of the third ethene molecule with the $\mu_4\text{-}C_2(CHCH_2)CHMe$ ligand of **4**. Complexes **4a**, **5b** and **8** were characterised by single-crystal X-ray studies.

1. Introduction

We recently described reactions between ethene or 1,3-butadiene and $Ru_5(\mu_5\text{-}C_2PPh_2)(\mu\text{-}PPh_2)(CO)_{13}$ (**1**; Scheme 1) to give the tetranuclear complexes $Ru_4\{\mu_4\text{-}\sigma(O,P),\eta^1,\eta^2\text{-}C_5H_4(O)(PPh_2)\}(\mu\text{-}PPh_2)(CO)_{11}$ (**2**) and $Ru_4\{\mu_4\text{-}\sigma(O,P),\eta^1,\eta^2\text{-}C_6H_3(CO)(PPh_2)\}(\mu\text{-}PPh_2)(CO)_{10}(\eta^3\text{-}C_4H_7)$ (**3**) respectively, which contain organic ligands formed by condensation of the coordinated C_2PPh_2 ligand in **1** with CO and the alkene or diene [2]. The reaction with ethene also afforded two other complexes; the first exists in two isomeric forms, one of which has been fully characterized crystallographically as $Ru_5(\mu_4\text{-}PPh)\{\mu_4\text{-}C_2(CHCH_2)CHMe\}(\mu\text{-}PPh_2)(CO)_{12}$ (**4a**). Fortuitously, the reaction with propene gave both analogous complexes (**5a** and **5b**), of which isomer **5b** could be studied crystallographically. Similar compounds (**6a** and **6b**) were also obtained from 1-butene. In the case of ethene and propene, the formation of **4** and **5** is competitive with that of **2** and its methyl homologue, **7**. The second complex obtained from the ethene reaction was identified crystallograph-

---

Correspondence to: Professor M.I. Bruce.

* For Part LXXXII, see ref. 1.

0022-328X/93/$6.00

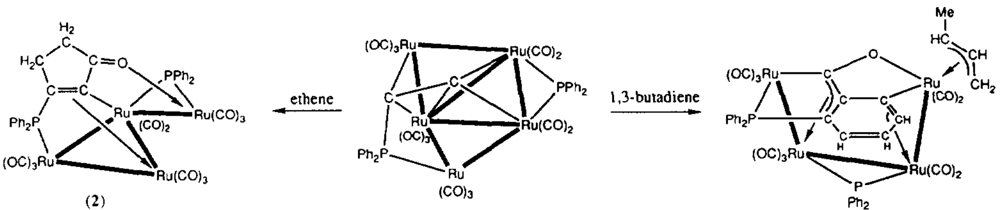

Scheme 1.

ically as $Ru_5(\mu_4\text{-PPh})(\mu\text{-PPh}_2)(\mu\text{-CO})(CO)_{10}\{\eta^5\text{-}C_5H_3Me\text{-}1\text{-}(CH{=}CH_2)\text{-}3\}$ (**8**). These complexes all contain ligands formed by oligomerisation of two or three molecules of the alkene with the C_2 fragment resulting from cleavage of the P–C(sp) bond in the C_2PPh_2 group.

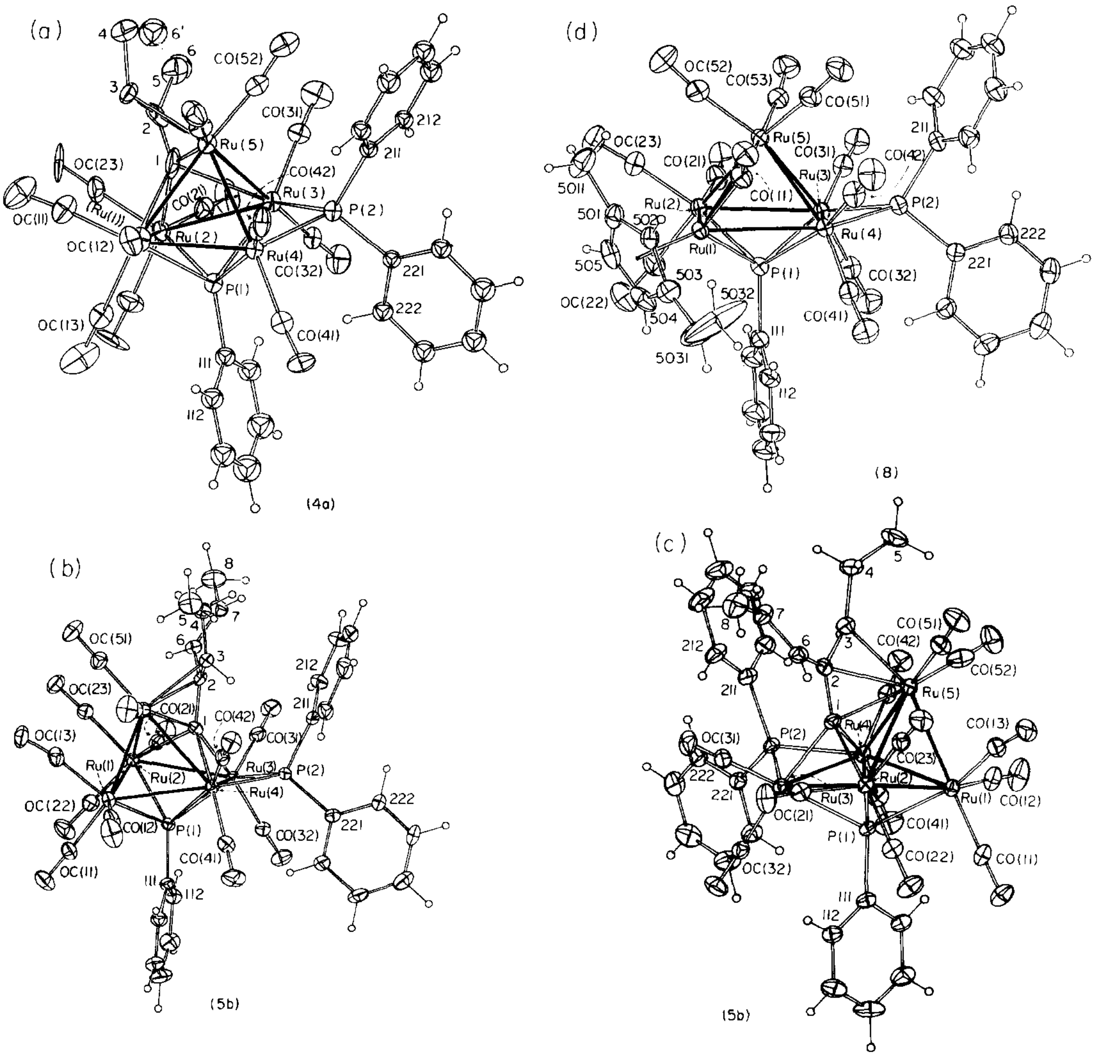

Fig. 1. (a) ORTEP diagram [23] of a molecule of $Ru_5(\mu_4\text{-PPh})\{\mu_4\text{-CC(CHCH}_2)(CHMe)\}(\mu\text{-PPh}_2)(CO)_{12}$ (**4a**), showing atom numbering scheme. Non-hydrogen atoms shown as 15% thermal ellipsoids; hydrogen atoms have arbitrary radii of 0.1 Å. (b) Plot of a molecule of $Ru_5(\mu_4\text{-PPh})\{\mu_4\text{-CC(CHCHMe)(CHEt)}\}(\mu\text{-PPh}_2)(CO)_{12}$ (**5b**), showing atom numbering scheme. (c) Alternative view of **5b** showing the 'butterfly' configuration of the basal Ru_4 unit. (d) Plot of a molecule of $Ru_5(\mu_4\text{-PPh})(\mu\text{-PPh}_2)(\mu\text{-CO})(CO)_{10}\{\eta^5\text{-}C_5H_3Me\text{-}1\text{-}(CH{=}CH_2)\text{-}3\}$ (**8**), showing atom numbering scheme.

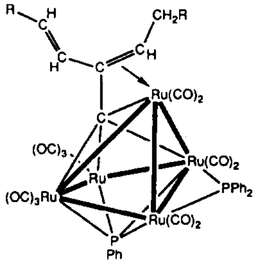

(4a) R = H
(5a) R = Me
(6a) R = Et

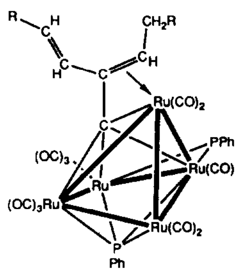

(4b) R = H
(5b) R = Me
(6b) R = Et

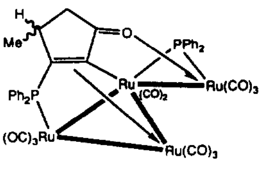

(7)

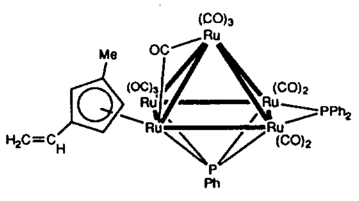

(8)

2. Results

Reactions involving the addition of the olefins ethene, propene or 1-butene to **1** have been investigated under a variety of conditions. The red tetraruthenium cluster $Ru_4\{\mu_4\text{-}\eta^2,O,P\text{-}C_5H_4(O)(PPh_2)\}(\mu\text{-}PPh_2)(CO)_{11}$ (**2**) [2] and two isomers of $Ru_5(\mu_4\text{-}PPh)\{\mu_4\text{-}\eta^3\text{-}C_2(CHCH_2)CHMe\}(\mu\text{-}PPh_2)(CO)_{12}$ [(**4a**) brown, (**4b**) red] were obtained from the thermal reaction between **1** and ethene under pressure. A reaction performed in an autoclave was checked at five hours, by which time the reaction was still incomplete and no other complexes were detected. A number of other minor products from these reactions were partially characterized by FAB MS and IR spectra (see Experimental section), but as their structures remain unknown at present, these complexes will not be discussed further.

Similar reactions were carried out with propene (toluene, Carius tube, 90°C, 4 d) and 1-butene (benzene, Carius tube, 87°C, 14 d). From the former, isomeric complexes **5a** and **5b** analogous to **4a** and **4b** were isolated, along with $Ru_4\{\mu_4\text{-}\sigma(O,P),\eta^1,\eta^2\text{-}MeC_5H_3(O)(PPh_2)\}(\mu\text{-}PPh_2)(CO)_{11}$ (**7**) and the pentanuclear carbido cluster $Ru_5(\mu_5\text{-}C)(\mu\text{-}C_4H_6PPh_2)(\mu\text{-}PPh_2)(CO)_{11}$ (**9**) which will be described elsewhere [3]. The 1-butene reaction gave as major products **6a** and **6b**, the expected analogues of **4a** and **4b**, together with several other minor products.

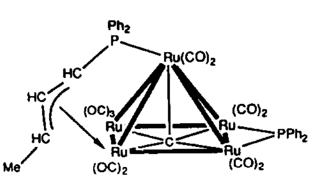

(9)

2.1. Molecular structures of $Ru_5(\mu_4\text{-}PPh)\{\mu_4\text{-}CC_2\text{-}CHCHR)CHCH_2R\}(\mu\text{-}PPh_2)(CO)_{12}$ [R = H (4a), Me (5b)]

X-ray structural studies have been performed on **4a** and **5b**. Plots of the two molecules are shown in Fig. 1(a, b), while selected bond distances and angles are given in Tables 1 and 2.

Neglecting the R groups, these two molecules are isomers, related by interchange of a $\mu\text{-}PPh_2$ group and two CO ligands. The metal skeleton approximates to a wing-tip-bridged butterfly; the butterflies are defined

TABLE 1. Selected bond distances (Å)

	4a	5b	8
Ru(5)–Ru(1)	2.935(1)	2.755(2)	2.857(1)
Ru(5)–Ru(2)		3.046(1)	2.807(2)
Ru(5)–Ru(3)	2.939(1)		2.919(1)
Ru(5)–Ru(4)	2.788(1)	2.939(2)	2.874(2)
Ru(1)–Ru(2)	2.824(1)	2.861(1)	2.845(1)
Ru(1)–Ru(4)	2.999(1)	2.963(1)	2.951(1)
Ru(2)–Ru(3)	2.962(1)	2.866(1)	2.911(1)
Ru(3)–Ru(4)	2.805(1)	2.775(2)	2.793(1)
P(1)–Ru(1)	2.383(3)	2.344(2)	2.296(2)
P(1)–Ru(2)	2.388(2)	2.373(2)	2.356(2)
P(1)–Ru(3)	2.422(3)	2.414(2)	2.377(2)
P(1)–Ru(4)	2.394(2)	2.414(2)	2.391(2)
P(2)–Ru(3)	2.302(2)	2.276(2)	2.266(2)
P(2)–Ru(4)	2.248(3)	2.298(2)	2.285(2)
C(1)–Ru(1)	2.43(1)		
C(1)–Ru(2)	2.19(1)	2.400(7)	
C(1)–Ru(3)	2.586(8)	2.090(8)	
C(1)–Ru(4)		2.314(7)	
C(1)–Ru(5)	1.96(1)	2.070(7)	
C(2)–Ru(5)	2.128(9)	2.180(7)	
C(3)–Ru(5)	2.266(8)	2.255(7)	
C(1)–C(2)	1.22(1)	1.42(1)	
C(2)–C(3)	1.47(1)	1.43(1)	

For 4a: Ru–CO, range 1.841(9)–1.97(1), av. 1.90
C–O, range 1.08–1.16(1), av. 1.14
P–C(Ph), range 1.808–1.826(5), av. 1.819
For 5b: Ru–CO, range 1.86(1)–1.922(8), av. 1.818
C–O, range 1.13–1.16(1), av. 1.14
P–C(Ph), range 1.811(7)–1.824(8), av. 1.816
For 8: Ru–CO, range 1.860–1.920(7), av. 1.889
C–O, range 1.12(1)–1.145(9), av. 1.138
P–C(Ph), range 1.815–1.828(6), av. 1.819
Ru(1)–C(501–5), 2.256(6), 2.229(6), 2.232(8), 2.168(8), 2.219(7)

TABLE 2. Selected bond angles (degrees)

Angles	4a	5b	8
Ru(4)-Ru(1)-Ru(2)	95.34(4)	79.50(2)	89.09(5)
Ru(1)-Ru(2)-Ru(3)	81.50(3)	96.25(3)	89.83(5)
Ru(2)-Ru(3)-Ru(4)	96.56(4)	82.64(3)	90.92(5)
Ru(3)-Ru(4)-Ru(1)	81.16(3)	95.98(3)	90.03(5)
Ru(5)-C(1)-Ru(1)	83.2(4)	-	
Ru(5)-C(1)-Ru(2)	144.4(5)	85.6(2)	
Ru(5)-C(1)-Ru(3)	79.2(3)	152.4(4)	
Ru(5)-C(1)-Ru(4)	-	84.0(2)	
Ru(1)-C(1)-C(2)	125.0(8)	-	
Ru(2)-C(1)-C(2)	135.2(9)	119.2(5)	
Ru(3)-C(1)-C(2)	129.4(9)	132.8(5)	
Ru(4)-C(1)-C(2)	-	128.9(5)	
Ru(5)-C(1)-C(2)	80.4(7)	74.8(4)	
Ru(1)-C(1)-Ru(3)	97.8(3)	-	
Ru(2)-C(1)-Ru(4)	-	104.4(3)	
C(1)-C(2)-C(3)	123 (1)	117.6(6)	

by Ru(1,3,4,5) and Ru(1,2,4,5), respectively. Figure 1(c) shows **5b** in an alternative orientation to display the skeleton in this aspect. The dihedral angles of the butterfly cores are 100.2° (**4a**; across Ru(1)-Ru(3)) and 129.88(5)° (**5b**; across Ru(2)-Ru(4)). The Ru-Ru separations range between 2.788(1)-2.999(1) Å (**4a**) and 2.755(2)-3.046(1) Å (**5b**).

The μ_4-PPh ligand caps one Ru_4 face [Ru(1)-Ru(2)-Ru(3)-Ru(4); Ru-P 2.383-2.422(3) Å (**4a**), 2.344-2.414(2) Å (**5b**)]. The metal skeletons are subtly different so that in **4a** there are three shorter Ru-P bonds, involving Ru(1), Ru(2) and Ru(4) [2.383(3), 2.388(2) and 2.394(2) Å respectively] and one longer bond to Ru(3) [2.422(3) Å]. In **5b** there are two shorter Ru-P bonds, to Ru(1) and Ru(2) [2.344(2) and 2.373(2) Å respectively] and two longer bonds, involving Ru(3) and Ru(4) [both 2.414(2) Å]. The Ru atoms coordinated to both P(1) and P(2) [Ru(3) and Ru(4)] have longer Ru-P(1) bond lengths than those Ru atoms which are coordinated only to P(1).

Atom C(1) caps the other Ru_4 face [Ru(1)-Ru(2)-Ru(3)-Ru(5) (**4a**); Ru(2)-Ru(3)-Ru(4)-Ru(5) (**5b**)] in asymmetric fashion [C(1)-Ru(1,2,3,5) 2.43(1), 2.19(1), 2.586(8), 1.96(1) (**4a**); C(1)-Ru(2,3,4,5) 2.400(7), 2.090(8), 2.314(7), 2.070(7) Å (**5b**)], being more distant from the hinge atoms; this difference is greater in **4a** than in **5b**, in which the more symmetrical approach to the face is reflected in the larger interplanar dihedral angle (see above). Inclusion of the Main Group elements in the cluster core defines a *closo*-pentagonal bipyramid [deviations of the atoms from the least-squares plane through Ru(3)P(1)Ru(1)Ru(5)C(1) in **5b** are −0.005(2), 0.074(5), 0.006(2), 0.003(2) and 0.12(2) Å respectively], with Ru(2) and Ru(4) symmetrically displaced above and below this plane [−2.145(2) and 2.217(2) Å respectively].

A μ-PPh_2 group bridges the Ru(3)-Ru(4) vector [Ru(3,4)-P(2) 2.303(2), 2.248(3) (**4a**); 2.276(2), 2.298(2)

TABLE 3. Crystal and refinement data for **4a**, **5b** and **8**

Compound	4a	5b	8
Formula	$C_{36}H_{22}O_{12}P_2Ru_5 \cdot H_2O$	$C_{38}H_{26}O_{12}P_2Ru_5$	$C_{37}H_{24}O_{11}P_2Ru_5 \cdot C_6H_{14}$
MW	1231.8	1241.9	1329.0
Crystal system	triclinic	monoclinic	triclinic
Space group	$P\bar{1}$ (No. 2)	$P2_1/c$ (No. 14)	$P\bar{1}$ (No. 2)
a, Å	10.814(2)	14.532(7)	18.989(11)
b, Å	20.157(3)	12.123(3)	12.624(6)
c, Å	9.882(1)	23.625(21)	10.041(7)
α, deg.	90.99(2)		98.65(5)
β, deg.	106.71(2)	98.40(6)	99.96(6)
γ, deg.	96.74(1)		96.63(4)
U, $Å^3$	2045.9	4118	2319
Z	2	4	2
D_c, g cm^{-3}	2.00	2.00	1.90
$F(000)$	1188	2400	1268
Crystal size, mm	0.25 × 0.34 × 0.36	0.28 × 0.21 × 0.35	0.17 × 0.05 × 0.40
A^* (min, max)	1.60, 1.94 (analytical)	1.40, 1.64 (gaussian)	1.09, 1.28 (gaussian)
μ, cm^{-1}	18.75	17.4	16.0
2θ limit, deg.	45	46	50
N_o unique data	5802	5516	8128
N_o data used	4102	4695	5624
R	0.045	0.037	0.034
R_w	0.052	0.043	0.036

Solvent atoms in **8** were refined as a rigid body group; the population of 1 was established by refinement.

TABLE 4. Non-hydrogen positional and isotropic displacement parameters (**4a**)

Atom	x	y	z	U_{eq} (Å^2)
Ru(1)	0.69326(8)	0.84660(4)	0.21217(8)	0.0423(3)
Ru(2)	0.85177(8)	0.89040(4)	0.04030(9)	0.0438(3)
Ru(3)	0.78664(7)	0.74828(4)	−0.06422(8)	0.0392(3)
Ru(4)	0.56974(7)	0.72027(4)	0.03667(8)	0.0375(3)
Ru(5)	0.81362(7)	0.72257(4)	0.23412(8)	0.0429(3)
C(11)	0.801(1)	0.8989(6)	0.375(1)	0.076(1)
O(11)	0.8603(9)	0.9327(6)	0.471(1)	0.123(1)
C(12)	0.593(1)	0.7911(5)	0.305(1)	0.061(1)
O(12)	0.5327(8)	0.7692(4)	0.3758(8)	0.079(1)
C(13)	0.579(1)	0.914(5)	0.177(1)	0.065(1)
O(13)	0.511(1)	0.9533(5)	0.161(1)	0.139(1)
C(21)	0.954(1)	0.8826(6)	−0.087(1)	0.068(1)
O(21)	1.0181(8)	0.8816(5)	−0.162(1)	0.103(1)
C(22)	0.780(1)	0.9723(6)	−0.034(1)	0.083(1)
O(22)	0.7439(9)	1.0186(5)	−0.070(1)	0.139(1)
C(23)	0.991(1)	0.9420(6)	0.185(1)	0.076(1)
O(23)	1.074(1)	0.9703(5)	0.273(1)	0.132(1)
C(31)	0.9384(8)	0.7095(5)	−0.060(1)	0.054(1)
O(31)	1.0255(7)	0.6862(5)	−0.067(1)	0.097(1)
C(32)	0.7724(9)	0.7647(5)	−0.2534(9)	0.047(1)
O(32)	0.7647(8)	0.7739(5)	−0.3679(8)	0.084(1)
C(41)	0.3951(9)	0.7192(5)	−0.085(1)	0.056(1)
O(41)	0.2909(6)	0.7121(5)	−0.1551(8)	0.079(1)
C(42)	0.5059(9)	0.6588(5)	0.1467(9)	0.051(1)
O(42)	0.4551(8)	0.6217(5)	0.2086(7)	0.079(1)
C(51)	0.7453(9)	0.6709(5)	0.362(1)	0.057(1)
O(51)	0.7131(8)	0.6406(5)	0.4470(9)	0.088(1)
C(52)	0.9050(8)	0.6538(5)	0.2108(9)	0.053(1)
O(52)	0.9697(7)	0.6129(5)	0.2075(8)	0.082(1)
P(1)	0.6410(2)	0.8268(1)	−0.0375(3)	0.0404(7)
C(111) [a]	0.5212(5)	0.8632(3)	−0.1760(5)	0.051(2)
C(112) [a]	0.3995(5)	0.8717(3)	−0.1610(5)	0.060(2)
C(113) [a]	0.3080(5)	0.8980(3)	−0.2697(5)	0.078(2)
C(114) [a]	0.3382(5)	0.9158(3)	−0.3834(5)	0.096(2)
C(115) [a]	0.4598(5)	0.9073(3)	−0.4084(5)	0.090(2)
C(116) [a]	0.5513(5)	0.8810(3)	−0.2997(5)	0.066(2)
P(2)	0.6425(2)	0.6517(1)	−0.0966(3)	0.0403(7)
C(211) [a]	0.7035(4)	0.5731(2)	−0.0476(5)	0.040(1)
C(212) [a]	0.7867(4)	0.5500(2)	−0.1173(5)	0.045(1)
C(213) [a]	0.8363(4)	0.4897(2)	−0.0822(5)	0.062(2)
C(214) [a]	0.8027(4)	0.4526(2)	0.0227(5)	0.065(2)
C(215) [a]	0.7195(4)	0.4757(2)	0.0924(5)	0.068(2)
C(216) [a]	0.6699(4)	0.5360(2)	0.0573(5)	0.050(2)
C(221) [a]	0.5310(5)	0.6279(2)	−0.2724(5)	0.041(1)
C(222) [a]	0.4764(5)	0.6781(2)	−0.3564(5)	0.053(2)
C(223) [a]	0.3813(5)	0.6611(2)	−0.4854(5)	0.065(2)
C(224) [a]	0.3409(5)	0.5940(2)	−0.5302(5)	0.072(2)
C(225) [a]	0.3955(5)	0.5439(2)	−0.4462(5)	0.074(2)
C(226) [a]	0.4906(5)	0.5609(2)	−0.3173(5)	0.054(2)
C(1)	0.889(1)	0.8083(6)	0.1830(8)	0.100(1)
C(2)	0.9810(9)	0.7956(5)	0.279(1)	0.060(1)
C(3)	0.9694(9)	0.7776(5)	0.4192(9)	0.056(1)
C(4)	1.063(1)	0.7411(7)	0.527(1)	0.091(1)
C(5)	1.107(1)	0.7849(7)	0.252(1)	0.080(1)
C(6) [a,b]	1.175(2)	0.812(1)	0.189(2)	0.093(2)
C(6′) [a,b]	1.222(2)	0.803(1)	0.307(2)	0.099(2)
O(0w)	0.0282(8)	0.4515(4)	0.4097(9)	0.085(1)

[a] Isotropic thermal parameters. [b] Site occupancy factor = 0.5.

TABLE 5. Non-hydrogen positional and isotropic displacement parameters (**5b**)

Atom	x	y	z	U_{eq} (Å^2)
Ru(1)	0.87548(4)	0.49812(5)	0.66414(3)	0.0409(2)
Ru(2)	0.68933(4)	0.48414(5)	0.60515(2)	0.0367(2)
Ru(3)	0.64312(4)	0.28087(5)	0.65620(2)	0.0339(2)
Ru(4)	0.83499(4)	0.26208(5)	0.68164(2)	0.0359(2)
Ru(5)	0.85470(4)	0.36043(5)	0.57036(3)	0.0434(2)
C(11)	0.8686(6)	0.6270(7)	0.7086(3)	0.055(3)
O(11)	0.8643(5)	0.7067(5)	0.7342(3)	0.083(3)
C(12)	0.9940(6)	0.4594(7)	0.7025(4)	0.066(4)
O(12)	1.0658(5)	0.4413(6)	0.7257(3)	0.104(3)
C(13)	0.9169(6)	0.5739(7)	0.6011(4)	0.059(3)
O(13)	0.9402(5)	0.6315(5)	0.5678(3)	0.081(3)
C(21)	0.5597(6)	0.4636(7)	0.5795(3)	0.054(3)
O(21)	0.4824(4)	0.4657(6)	0.5628(3)	0.083(3)
C(22)	0.6668(6)	0.6214(7)	0.6372(3)	0.055(3)
O(22)	0.6558(5)	0.7038(5)	0.6573(3)	0.084(3)
C(23)	0.7133(5)	0.5521(7)	0.5353(3)	0.050(3)
O(23)	0.7203(4)	0.5995(5)	0.4948(3)	0.073(3)
C(31)	0.5415(6)	0.2305(7)	0.6039(3)	0.053(3)
O(31)	0.4783(4)	0.2052(6)	0.5715(2)	0.076(3)
C(32)	0.5705(5)	0.2744(6)	0.7177(3)	0.048(3)
O(32)	0.5270(4)	0.2668(5)	0.7536(3)	0.075(3)
C(41)	0.8874(5)	0.2494(6)	0.7592(4)	0.053(3)
O(41)	0.9211(5)	0.2434(6)	0.8056(3)	0.087(3)
C(42)	0.9363(6)	0.1783(6)	0.6634(3)	0.048(3)
O(42)	0.9972(4)	0.1238(5)	0.6566(3)	0.074(3)
C(51)	0.8712(6)	0.4256(7)	0.5004(4)	0.060(3)
O(51)	0.8774(5)	0.4629(6)	0.4574(3)	0.090(3)
C(52)	0.9825(8)	0.3359(7)	0.5814(4)	0.074(4)
O(52)	1.0620(4)	0.3201(6)	0.5878(3)	0.094(3)
P(1)	0.7462(1)	0.4235(2)	0.69929(7)	0.0357(6)
C(111)	0.7173(5)	0.4795(6)	0.7656(3)	0.044(3)
C(112)	0.6276(6)	0.5097(6)	0.7715(3)	0.053(3)
C(113)	0.6104(7)	0.5558(8)	0.8223(4)	0.072(4)
C(114)	0.6806(9)	0.5746(9)	0.8668(4)	0.084(5)
C(115)	0.7698(7)	0.5456(8)	0.8607(3)	0.073(4)
C(116)	0.7879(6)	0.4978(6)	0.8116(3)	0.053(3)
P(2)	0.7261(1)	0.1243(2)	0.68027(7)	0.0370(6)
C(211)	0.7335(6)	0.0164(6)	0.6273(3)	0.051(3)
C(212)	0.6667(7)	0.0016(7)	0.5804(3)	0.068(4)
C(213)	0.680(1)	−0.077(1)	0.5393(4)	0.097(5)
C(214)	0.758(1)	−0.1395(9)	0.5460(5)	0.105(7)
C(215)	0.8244(9)	−0.1270(8)	0.5921(6)	0.097(6)
C(216)	0.8130(6)	−0.0491(7)	0.6325(4)	0.065(4)
C(221)	0.7096(5)	0.0482(6)	0.7441(3)	0.046(3)
C(222)	0.6943(6)	−0.0637(7)	0.7437(3)	0.055(3)
C(223)	0.6842(7)	−0.1179(7)	0.7930(4)	0.076(4)
C(224)	0.6878(8)	−0.063(1)	0.8437(4)	0.085(5)
C(225)	0.7024(8)	0.0484(9)	0.8457(3)	0.082(4)
C(226)	0.7130(6)	0.1042(7)	0.7957(3)	0.060(3)
C(1)	0.7366(5)	0.2957(6)	0.5973(3)	0.041(3)
C(2)	0.7387(5)	0.2499(6)	0.5422(3)	0.042(3)
C(3)	0.8206(6)	0.1917(6)	0.5329(3)	0.050(3)
C(4)	0.8465(7)	0.1557(7)	0.4768(4)	0.070(4)
C(5)	0.9478(7)	0.1405(9)	0.4764(5)	0.098(5)
C(6)	0.6628(6)	0.2725(7)	0.4949(3)	0.052(3)
C(7)	0.6279(6)	0.1989(7)	0.4553(3)	0.063(3)
C(8)	0.5477(7)	0.2213(9)	0.4102(4)	0.093(5)

Å (**5b**)], more symmetrically in the latter. There are 12 CO groups on the five metal atoms: Ru(1) and Ru(2) have three each, while the other metal atoms have two CO ligands each. In **4a**, CO(12) semi-bridges the Ru(1)–Ru(4) vector [Ru(1)–C(12) 1.89(1), Ru(4)–C(12) 2.92(1) Å; Ru(1)C(12)O(12) 166.2(9)°].

Of most interest is the organic ligand that has been formed by combination of two molecules of the olefin with the C_2 fragment formed by cleavage of the P–C bond in **1**. As mentioned above, in both cases C(1) spans the Ru_4 face in an asymmetric fashion. In **4a** the interaction with Ru(3) is rather long, but there is likely to be a weak bonding interaction, as there is a formal electron deficiency at this ruthenium (17e). To this methylidyne carbon is attached a buta-1,3-dien-2-yl substituent which has in addition, 1-Me (**4a**) or 1-Et and 4-Me (**5b**) substituents. An η^3 interaction between C(1)C(2)C(3) and Ru(5) in both complexes [Ru(5)–C(1,2,3) 1.96(1), 2.128(9), 2.266(8) Å (**4a**); 2.070(7), 2.180(7), 2.255(7) Å (**5b**)] is necessary to fulfil the electronic requirements of this metal atom.

Within the organic group of **5b**, there are both C–C single bonds [C(2)–C(6) 1.48(1), C(3)–C(4) 1.50(1), C(4)–C(5) 1.48(1), C(7)–C(8) 1.49(1) Å] and C=C double bonds [C(1)–C(2) 1.42(1), C(2)–C(3) 1.43(1), C(6)–C(7) 1.34(1) Å]. A similar pattern of bond lengths in the analogous ligand of **4a** is presumed [C(1)–C(2) 1.22(1), C(2)–C(3) 1.47(1), C(2)–C(5) 1.51(2), C(5)–C(6,6′) 1.18(2), 1.21(2), C(6)–C(6′) 1.16(2), C(6)–C(7) 1.36(2) Å], but the interpretation is severely compromised by the disorder found for C(6), which takes up two positions related by rotation of the vinyl group about the C(2)–C(5) vector. The whole organic ligand supplies five electrons to the cluster, which achieves an electron-precise count from the other ligands present and the seven Ru–Ru bonds. Both clusters have 76-electron, 8-SEP electron counts.

The IR spectra of these complexes have all-terminal ν(CO) band patterns, together with a band at 1532 cm^{-1} which is probably associated with the delocalised system in the organic ligand.

The ^1H NMR spectrum of **4a** contains resonances at δ 1.64 (H(3) and CH_3), 5.33 (H(6c)), 5.54 (H(5)) and 5.59 (H(6t)). Vicinal coupling constants indicate that H(6c) is *cis* to H(5) (^3J(HH) 10.2 Hz) and H(6t) is *trans* to H(5) (^3J(HH) 17.5 Hz). In **4b** these protons resonate at δ 0.61, 1.28, 5.19, 5.09 and 4.97 respectively. The ^1H NMR spectrum of **5a** contains resonances at δ 1.06 (H(5)), 1.53 (H(3)), 1.72 (H(8)), 1.88 (H(4)), 5.20 (H(6)) and 6.21 (H(7)). In **5b** these protons resonate at δ 0.81, 0.64, 1.63, 1.41, 4.78 and 5.35 respectively. The ^{13}C NMR spectrum of **4a** contains resonances at δ 17.19 (Me), 51.23 (C(3)), 120.35 (C(6)) and 136.94(C(5)). In **4b** these carbons resonate at δ 17.69, 53.37, 121.16 and 137.24, respectively. The ^{13}C NMR spectrum of **5b** contains resonances at δ 16.49 and 18.37 (Me), 25.62 (C(4)) and 63.56 (C(3)). The C(6) and C(7) resonances are obscured by the Ph resonances. A peak at δ 111.28 is assigned to C(2). The resonances for the methylidyne carbons, C(1), were either not observed or located in the CO region. The ^{31}P NMR spectra of **4a** and **4b** contain similar phosphido and phosphinidene environments at δ 236.7, 353.4 (**4a**) and δ 232.6, 374.3 (**4b**), with phosphorus–phosphorus coupling being observed in each case.

The FAB mass spectra for all the Ru_5 complexes contained molecular ions which were fragmented by the loss of CO groups. Because of the similar nominal masses of CO and C_2H_4, and of 2CO and C_4H_8, the exact nature of the fragmentations could not be determined from low-resolution spectra.

An investigation of the isomer pair **4a**/**4b** has shown that the former slowly isomerises when the solids are dissolved in cyclohexane. The reaction is not significantly affected by the presence of ethene. No exchange was found to take place between 1-butene and isomer **4b** after 15 days in solution. These results suggest that intramolecular rearrangements occur in solution to give structurally-related isomers, as exemplified by **4a** and **5b**.

When ethene was passed through a solution of (**1**) in hot cyclohexane, a further complex, $Ru_5(\mu_4\text{-}PPh)(\mu\text{-}PPh_2)(\mu\text{-}CO)(CO)_{10}\{\eta^5\text{-}C_5H_3Me\text{-}1\text{-}(CH{=}CH_2)\text{-}3\}$ (**8**), was obtained as a minor product, together with **4a** and **4b**. Complex **4a** could be converted into **8** under conditions similar to those used in the direct synthesis of **8** from **1**. The identity of **8** was determined by a single crystal X-ray study.

2.2. *Molecular structure of $Ru_5(\mu_4\text{-}PPh)(\mu\text{-}PPh_2)(\mu\text{-}CO)(CO)_{10}\{\eta^5\text{-}C_5H_3Me\text{-}1\text{-}(CH{=}CH_2)\text{-}3\}$ (8)*

A plot of a molecule of **8** is shown in Fig. 1(d) and selected bond distances and angles are given in Tables 1 and 2. Complex **8** has a distorted square-pyramidal Ru_5 core, to the Ru_4 face of which is attached the phosphinidene P(1) atom, which is situated 1.187 Å below the square base; Ru(5) is 2.017 Å above it. The eight Ru–Ru bonds are in the range 2.793(1)–2.951(1) Å. The phosphinidene ligand is attached to the basal Ru atoms by one short [Ru(1)–P(1) 2.296(2) Å] and three longer bonds [Ru(2,3,4)–P(1) 2.356(2), 2.377(2), 2.391(2) Å]; the μ-PPh_2 group bridges Ru(3)–Ru(4) [Ru(3,4)–P(2) 2.266(2), 2.285(2) Å]. A 1-methyl-3-vinylcyclopentadienyl ligand is almost symmetrically bound to Ru(1) [Ru–C distances 2.171(7)–2.256(6) Å], and within the cyclopentadienyl ligand the C–C separations are between 1.40(1) and 1.43(1) Å. The C(5031)–C(5032) bond distance [1.22(2) Å] suggests

TABLE 6. Non-hydrogen positional and isotropic displacement parameters (**8**)

Atom	*x*	*y*	*z*	U_{eq} (Å^2)
Ru(1)	0.08619(2)	0.25761(4)	−0.13141(5)	0.0432(2)
Ru(2)	0.17877(3)	0.17177(4)	−0.30126(5)	0.0447(2)
Ru(3)	0.30407(2)	0.27962(4)	−0.09605(5)	0.0404(2)
Ru(4)	0.21491(2)	0.37427(4)	0.06674(5)	0.0423(2)
Ru(5)	0.19268(3)	0.39679(4)	−0.21752(5)	0.0444(2)
C(11)	0.1005(3)	0.4128(6)	−0.0898(7)	0.067(3)
O(11)	0.0734(3)	0.4920(4)	−0.0666(6)	0.082(2)
C(21)	0.2556(4)	0.1590(6)	−0.3979(7)	0.070(3)
O(21)	0.2967(3)	0.1475(5)	−0.4661(5)	0.100(3)
C(22)	0.1488(4)	0.0207(6)	−0.3274(8)	0.079(3)
O(22)	0.1260(4)	−0.0688(4)	−0.3490(7)	0.135(3)
C(23)	0.1098(4)	0.1850(6)	−0.4550(7)	0.071(3)
O(23)	0.0677(3)	0.1843(5)	−0.5503(5)	0.107(3)
C(31)	0.3787(3)	0.3014(6)	−0.1962(6)	0.060(3)
O(31)	0.4254(2)	0.3102(4)	−0.2525(5)	0.083(2)
C(32)	0.3581(3)	0.1832(5)	−0.0178(7)	0.062(3)
O(32)	0.3932(3)	0.1266(4)	0.0310(6)	0.094(3)
C(41)	0.2056(3)	0.3365(6)	0.2354(7)	0.066(3)
O(41)	0.2008(3)	0.3194(5)	0.3416(5)	0.099(3)
C(42)	0.1987(4)	0.5127(6)	0.1410(7)	0.072(3)
O(42)	0.1881(3)	0.5957(4)	0.1877(6)	0.110(3)
C(51)	0.2154(4)	0.5461(5)	−0.1398(7)	0.069(3)
O(51)	0.2286(3)	0.6372(4)	−0.1014(6)	0.102(3)
C(52)	0.1240(4)	0.4209(6)	−0.3675(8)	0.077(3)
O(52)	0.0852(3)	0.4439(6)	−0.4552(6)	0.127(3)
C(53)	0.2670(3)	0.4037(6)	−0.3175(7)	0.065(3)
O(53)	0.3069(3)	0.4204(4)	−0.3887(5)	0.088(2)
P(1)	0.19235(8)	0.1938(1)	−0.0605(2)	0.0467(6)
C(111)	0.1955(3)	0.0775(5)	0.0260(7)	0.055(2)
C(112)	0.1682(3)	0.0724(5)	0.1435(7)	0.066(3)
C(113)	0.1739(4)	−0.0149(7)	0.2112(8)	0.089(4)
C(114)	0.2076(5)	−0.0988(7)	0.159(1)	0.107(4)
C(115)	0.2346(5)	−0.0957(6)	0.0424(9)	0.096(4)
C(116)	0.2290(4)	−0.0079(6)	−0.0237(8)	0.074(3)
P(2)	0.33714(9)	0.4155(1)	0.0875(2)	0.0493(6)
C(211)	0.3739(3)	0.5536(5)	0.0760(6)	0.052(2)
C(212)	0.3692(4)	0.6380(5)	0.1787(7)	0.067(3)
C(213)	0.3926(4)	0.7422(5)	0.1710(8)	0.077(3)
C(214)	0.4230(4)	0.7651(6)	0.0615(8)	0.085(4)
C(215)	0.4291(4)	0.6829(6)	−0.0390(8)	0.083(3)
C(216)	0.4038(4)	0.5770(5)	−0.0336(7)	0.066(3)
C(221)	0.3989(3)	0.3884(5)	0.2335(6)	0.050(2)
C(222)	0.4684(3)	0.4451(5)	0.2753(7)	0.061(3)
C(223)	0.5171(4)	0.4166(6)	0.3770(8)	0.075(3)
C(224)	0.4975(4)	0.3335(7)	0.4413(7)	0.081(3)
C(225)	0.4287(4)	0.2764(7)	0.4013(7)	0.079(3)
C(226)	0.3806(3)	0.3027(6)	0.2981(7)	0.070(3)
C(501)	−0.0282(3)	0.2357(6)	−0.2506(7)	0.070(3)
C(5011)	−0.0585(4)	0.2860(9)	−0.3710(8)	0.115(5)
C(502)	−0.0268(3)	0.2786(5)	−0.1110(7)	0.059(3)
C(503)	−0.0020(3)	0.2047(6)	−0.0242(7)	0.075(3)
C(5031)	−0.0038(5)	0.211(1)	0.1237(9)	0.136(6)
C(5032)	−0.023(1)	0.288(1)	0.190(1)	0.31(1)
C(504)	0.0126(4)	0.1168(6)	−0.1165(9)	0.089(4)
C(505)	−0.0038(4)	0.1342(6)	−0.2526(9)	0.087(3)
C(01) [a]	0.4704(9)	0.989(2)	0.697(2)	0.41(2)
C(02) [a]	0.4103(8)	0.939(1)	0.615(1)	0.47(2)
C(03) [a]	0.3531(9)	0.911(1)	0.705(2)	0.41(2)
C(04) [a]	0.3185(8)	0.814(1)	0.643(1)	0.44(2)
C(05) [a]	0.2809(9)	0.776(2)	0.519(1)	0.59(3)
C(06) [a]	0.265(1)	0.682(1)	0.546(2)	0.34(1)

[a] Refined as rigid body with isotropic thermal parameter.

that the ring substituent at this position may be a vinyl group but thermal motion here is very high and the apparent shortness of this distance may be an illusion due to libration effects. The eleven carbonyl groups are attached two to each of Ru(3) and Ru(4), and three to each of Ru(2) and Ru(5); one CO group asymmetrically bridges the Ru(1)–Ru(5) bond [Ru(1)–C(11) 1.917(7), Ru(5)–C(11) 2.351(8) Å; Ru(5)C(51)O(51) 124.9(6)°] with a rather short non-bonding distance to Ru(4) [Ru(4) $\cdots$ C(11) 2.595(7) Å]. A semi-bridging carbonyl is also present between Ru(5) and Ru(3) [Ru(5)C(53)O(53) 168.8(6)°, Ru(3) $\cdots$ C(53) 2.945(8) Å]. Complex **8** has a 74-electron, 7-SEP electron count.

3. Discussion

The original objective for the reactions which led to the formation of **1** was to make ruthenium cluster complexes containing the all-carbon ligand C_2 by cluster-mediated cleavage of the two P–C(sp) bonds in the dppa ligand. This has been achieved independently in reactions of **1** with CO [4], pyridine [5] or Me_2S_2 [6]. In the present work, the structures of the products **4** and **5** (and by analogy, that of **6**) indicate that cleavage of the remaining P–C(sp) bond in **1** has occurred, but that the C_2 fragment has been incorporated into the $C_2(CHCHR)(CHCH_2R)$ (R = H, Me, Et) ligands by combination with two molecules of the respective olefins. Further alteration of a PPh_2 group in **1** occurs by loss of Ph to give a μ_4-PPh group.

$$C_2PPh_2 + PPh_2 + 2CH_2{=}CHR \rightarrow C_2(CHCHR)(CHCH_2R) + PPh + PPh_2 + C_6H_6$$

It has not been possible to determine the order of these reactions, the source of the PPh group (from the PPh_2 or the C_2PPh_2 ligands in **1**), nor the fate of the Ph group. Presumably the latter is lost as C_6H_6 by combination with the stoichiometrically-required H atom derived from the olefin. We have not detected any intermediate containing only one olefin molecule: the cycloadduct **2** is shown not to be an intermediate by its lack of further reaction with ethene under conditions where **4** was formed from **1**.

There is an interesting difference between the X-ray-determined molecular structures of the ethene and propene products, wherein the μ-PPh_2 and μ-CO groups are interchanged relative to the geometry of the Ru_5 skeleton. The IR spectra are consistent with the two structurally characterised products being the two isomers seen in solution by NMR spectroscopy. Consideration of possible isomerisation pathways leads to our suggestion that **4a** (**5a**) is converted to **4b** (**5b**) by a simple migration of CO and μ-PPh_2 groups around

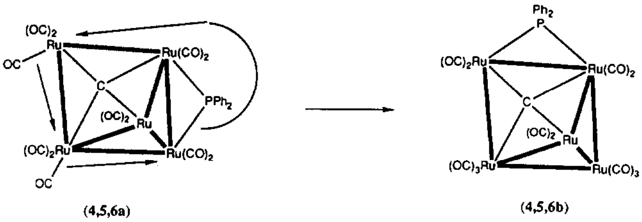

Scheme 2.

the square perimeter of the PRu$_5$ skeleton. This can be achieved by opening of the PR$_2$ bridge with concomitant formation of a bridging CO group, followed by closing of the PR$_2$ bridge to the adjacent Ru atom and opening of the CO bridge (Scheme 2), as has been observed in other related systems [7]. These isomers are not in equilibrium, NMR studies showing that while pure **4a** slowly isomerises to **4b** in solution over a period of days, no similar change occurs with pure **4b**.

Formation of **8** by addition of the third ethene molecule to the C$_2$(CHCH$_2$)(CHMe) ligand in **4** is accompanied by loss of two H atoms, a carbonyl ligand and major structural rearrangement in the metal core. Ruthenium clusters containing cyclopentadienyl ligands are relatively rare. The only pentanuclear clusters noted to date are Ru$_5$(CO)$_6$(η-C$_5$H$_5$)$_4$ [8] and AuRu$_5$-C(CO)$_{13}$(PPh$_3$(η-C$_5$H$_5$) [9] while some smaller clusters are mentioned in a review on ruthenium and osmium complexes containing η^5-dienyl ligands [10a] or were reported recently [10b]. The reaction is complex; 'simple' cycloaddition reactions lead to cyclopentadienyl groups with the wrong substituent pattern. However, a formal route to **8** is shown in Scheme 3; formation of vinylidene from ethene has been described in reactions of Os$_3$(CO)$_{12}$ [11].

The alkene–acetylide coupling reactions examined here are without precedent in cluster chemistry and are therefore of considerable interest. Reactions of ethene with clusters have generally given η^2-bonded complexes [12], while the reactions of Ru$_3$(CO)$_{12}$ with ethene have been shown to give C–C coupled products such as Ru$_4$(μ_4-η^2-C$_2$Me$_2$)(CO)$_{12}$ and Ru$_6$(C(μ-η^2,η^2-MeCH=CHCH=CHMe)(μ-CO)(CO)$_{14}$ formed by oligomerisation of the olefin [13]. Clusters **2–9** may be seen as model compounds for C–C bond-forming reactions which occur at metal surfaces [14].

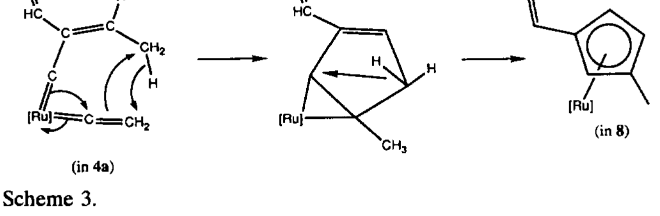

Scheme 3.

Although the formation of two-carbon fragments during the Fischer–Tropsch reaction must occur, this process is generally assumed to proceed by coupling of surface-bound CH$_2$ groups [15]. In a survey of possible Fischer–Tropsch reaction mechanisms, formation of MCCM species was considered to be a special case of the more general reaction:

$$\text{M-C}_n\text{H}_m + \text{M-C}_r\text{H}_s \rightarrow \text{M-C}_{n+r}\text{H}_{m+s} + \text{M}$$

and supposed to be an intermediate step in the formation of the carbon (graphite) deposits which deactivate Fischer–Tropsch catalysts [15c]. Two-carbon intermediates have been implicated in the carbon–carbon chain growth process of Fischer–Tropsch catalysis [16]. However, little is known about the reactivity of these species.

The conversion of the cluster-bonded methylidyne to a cyclic system in going from **4** to **8** is also of interest in relevance to Fischer–Tropsch chemistry. Reaction of C$_2$ fragments (either 'naked' or as olefins) have, in this case, not led to long chain hydrocarbons. This is probably as a result of the considerable unsaturation remaining in the organic ligands present in **4–6**; further reaction with olefin generates a system which relieves unsaturation by cyclisation rather than chain extension.

4. Conclusions

The results presented above suggest that the C$_2$ fragment associated with a molecular metal cluster is highly reactive and in our system, at least, if C$_2$ is formed as an intermediate, it does not exhibit any tendency to form higher carbon aggregates. A similar conclusion can be drawn from our on-going examination of the reactions of cluster complexes which do contain C$_2$ ligands [17]. However, it must also be said that electronic modification of an Ru$_5$C$_2$ fragment by the presence of carbonyl, phosphorus and other ligands may considerably reduce the utility of these systems as models of the surface-bound C$_2$ molecule. This chemistry has also shown that acetylide–alkene coupling is also a facile process for transition-metal cluster complexes.

5. Experimental details

5.1. General conditions

All reactions were carried out under dry, high purity nitrogen by use of standard Schlenk techniques. Solvents were dried and distilled before use. Elemental analyses were by the Canadian Microanalytical Service, Delta, B.C., Canada V4G 1G7. TLC was carried out on glass plates (20 × 20 cm) coated with silica gel (Merck 60 GF_{254}, 0.5 mm thick).

Reagents Complex **1** was prepared by the literature method [18]. $Me_3NO \cdot 2H_2O$ (Aldrich) was dehydrated by sublimation (100°C (0.1 mm^{-1})). Ethene (Commonwealth Industrial Gases), propene (J.T. Baker) and but-1-ene (Fluka) were used as received.

Instrumentation. IR: Perkin-Elmer 683 double beam and 1720X FT spectrometers, NaCl optics, calibrated using polystyrene absorption at 1601.4 cm^{-1}; NMR: Bruker CXP300 and ACP300 spectrometers (^1H NMR at 300.13 MHz, ^{13}C NMR at 75.47 MHz, ^{31}P NMR at 121.49 MHz); ^{31}P chemical shifts are relative to external 85% H_3PO_4. Spectra recorded in non-deuterated solvents used an external concentric tube containing D_2O for field lock. FAB MS: VG ZAB 2HF (FAB MS, using 3-nitrobenzyl alcohol as matrix, exciting gas Ar, FAB gun voltage 7.5 kV, current 1 mA, accelerating potential 7 kV).

5.2. Reactions between 1 and ethene

5.2.1. Under pressure (20 atm)

A solution of **1** (200 mg, 0.158 mmol) in benzene (15 ml) was placed in a small autoclave (100 ml) and pressurised to 20 atm with ethene. After being kept at 80°C for 8.5 h the mixture was cooled (pressure had dropped to 10 atm) and the orange solution then evaporated to dryness under reduced pressure. Preparative TLC (petroleum ether/acetone 9/1) of the residue gave ten bands of which the major three were collected. A brown band (R_f 0.59) was crystallized (CH_2Cl_2/petroleum ether) as **4a** (27 mg, 0.022 mmol, 14%), m.p. 209–210°C. (Found: C, 33.97; H, 1.84; M, 1214 (mass spectrometry). $C_{36}H_{22}O_{12}P_2Ru_5 \cdot CH_2Cl_2$ calcd.: C, 34.18; H, 1.85%; M, 1214.) IR (cyclohexane): ν(CO) 2079m, 2048m, 2030(sh), 2024s, 2013s, 1997m, 1978(sh), 1971m, 1958w, 1952w cm^{-1}. ^1H NMR ($CDCl_3$): δ 1.64 (4H, m, H(3) and Me), 5.33 (1H, dd, *J*(HH) 10.2, 1.8 Hz, H(6c)), 5.54 (1H, dd, *J*(HH) 17.4, 10.3 Hz, H(5)), 5.59 (1H, dd, *J*(HH) 17.5, 1.8 Hz, H(6t)), 6.30 (2H, dd, *J*(HH) 7.9, 12.9 Hz, Ph), 6.88 (2H, t, *J*(HH) 7.0 Hz, Ph), 7.06 (1H, t, *J*(HH) 6.84 Hz, Ph), 7.41–7.63 (8H, m, Ph), 8.07 (2H, dd, *J*(HH) 12.5, 7.4 Hz, Ph). ^{13}C NMR ($CDCl_3$): δ 17.29 (s, Me), 51.23 (s, C(3)), 120.35 (s, C(6)); 127.30–133.90 (m, Ph), 136.94 (s, C(5)). FAB MS: 1214, $[M - H]^+$; loss of 12 CO groups.

An orange band (R_f 0.47) was removed from the silica with CH_2Cl_2 (−15°C) and crystallized (CH_2Cl_2/petroleum ether) quickly to give orange plate-like crystals of **4b** (43 mg, 0.035 mmol, 22%), m.p. 173–174°C. (Found: C, 35.17; H, 1.83; M, 1214 (mass spectrometry). $C_{36}H_{22}O_{12}P_2Ru_5$ calcd.: C, 35.58; H, 1.81%; M, 1214.) IR (cyclohexane): ν(CO) 2070m, 2042(sh), 2037s, 2023s, 2016s, 1984(sh), 1975w, 1958w cm^{-1}. IR (CH_2Cl_2): ν(CO) 1532 cm^{-1}. ^1H NMR ($CDCl_3$): δ 0.61 (1H, q, *J*(HH) 6.1 Hz, H(3)), 1.28 (3H, d, *J*(HH) 6.1 Hz, Me), 4.97 (1H, dd, *J*(HH) 17.1, 2.2 Hz, H(6t)), 5.09 (1H, dd, *J*(HH) 17.1, 10.4 Hz, H(5)), 5.19 (1H, dd, *J*(HH) 10.4, 2.2 Hz, H(6c)), 6.89–6.96 (2H, m, Ph), 7.18–7.28 (3H, m, Ph), 7.41–7.53 (6H, m, Ph), 7.65–7.72 (2H, m, Ph), 7.74–7.82 (2H, m, Ph). ^{13}C NMR ($CDCl_3$): δ 17.69 (s, Me), 53.37 (s, C(3)), 121.16 (s, C(6)), 128.00–134.06 (m, Ph), 137.24 (s, C(5)). FAB MS: 1214, $[M - H]^+$; loss of 12 CO groups, relative intensities similar to **4a**.

A red band (R_f 0.33) was removed from the silica quickly and crystallized (CH_2Cl_2/MeOH) by slow evaporation to give small red needles of **2** (31 mg, 0.027 mmol, 17%) [2].

5.2.2. In a Carius tube

A solution of **1** (150 mg, 0.12 mmol) in benzene (20 ml) was placed in a Carius tube (40 ml internal volume) and ethene (1.0 g, 35.7 mmol) was added. After being kept at 85°C for 24 h the solution was cooled and the excess of ethene vented. The solvent was removed under reduced pressure and the residue purified by preparative TLC (petroleum ether/acetone 9/1). Four bands were collected: (1) a yellow band (R_f 0.85) near the solvent front was identified (IR, spot TLC) as $Ru_3(CO)_{12}$ (4 mg, 0.006 mmol, 5%); the next three bands were identified (IR) as: (2) R_f 0.55, brown, **4a** (15 mg, 0.012 mmol, 10%); (3) R_f 0.45, orange, **4b** (22 mg, 0.018 mmol, 15%); (4) R_f 0.33, red, **2** (37 mg, 0.032 mmol, 27%). Five other minor bands and the brown base-line were not investigated.

5.3. Reaction between 1 and propene

A solution of **1** (200 mg, 0.158 mmol) and propene (2.6 g, 61.8 mmol) in toluene (10 ml) were heated in a Carius tube (40 ml) at 90°C for 4 d. The solvent was removed and the residue purified by preparative TLC (petroleum ether/acetone 4/1) to yield six major bands. A brown band (R_f 0.7) was recrystallised from CH_2Cl_2/MeOH to yield **5a** (24 mg, 12%), m.p. 139–142°C (decomposes). (Found: C, 35.79; H, 2.18; M, 1243 (mass spectrometry). $C_{38}H_{26}O_{12}P_2Ru_5 \cdot CH_2Cl_2$ calcd.: C, 35.26; H, 2.11%; M, 1243.) IR (cyclohexane): ν(CO) 2076m, 2045m, 2025vs, 2011s, 1992m, 1975(sh), 1967m, 1956w, 1948w cm^{-1}. ^1H NMR ($CDCl_3$): δ 1.06 (3H, t, *J*(HH) 7.3 Hz, H(5)), 1.53 (1H, t, *J*(HH) 6.4 Hz, H(3)), 1.72 (3H, dd, *J*(HH) 6.5, 1.5 Hz, H(8)), 1.88 (2H, dq, *J*(HH) 7.0, 7.3 Hz, H(4)), 5.20 (1H, dd, *J*(HH) 15.8, 1.6 Hz, H(6)), 6.21 (1H, dq, *J*(HH) 15.8, 6.6 Hz, H(7)), 6.28 (2H, dd, *J*(HH) 13.0, 7.9 Hz, Ph), 6.86 (2H, td, *J*(HH) 7.8, 2.0 Hz, Ph), 7.06 (1H, tm, *J*(HH) 6.8 Hz, Ph), 7.40–7.61 (8H, m, Ph), 8.06 (2H, dd, *J*(HH) 12.7, 7.6 Hz, Ph). FAB MS (*m/z*) 1243, $[M]^+$; loss of 12 CO groups.

A red band (R_f 0.6) was recrystallised from CH_2Cl_2/MeOH to yield **5b** (42 mg), 21%), m.p. 208–210°C (decomposes). (Found: C, 36.56: H, 2.12%; M, 1242 (mass spectrometry). $C_{38}H_{26}O_{12}P_2Ru_5$ calcd.: C, 36.71; H, 2.09%; M, 1242.) IR (cyclohexane): ν(CO) 2067m, 2035vs, 2019(sh), 2015vs, 2006m, 1994m, 1978(sh), 1968m, 1955w cm^{-1}. ^1H NMR ($CDCl_3$): δ 0.64 (1H, t, *J*(HH) 5.6 Hz, H(3)), 0.81 (3H, t, *J*(HH) 7.3 Hz, H(5)), 1.41 (2H, qd, *J*(HH) 7.3, 4.4 Hz, H(4)), 1.63 (3H, dd, *J*(HH) 6.5, 1.1 Hz, H(8)), 4.78 (1H, dd, *J*(HH) 15.7, 1.3, H(6)), 5.35 (1H, dq, *J*(HH) 15.7, 6.6 Hz, H(7)), 6.84–6.91 (2H, m, Ph), 7.16–7.24 (6H, m, Ph), 7.43–7.51 (3H, m, Ph), 7.67 (2H, m, Ph), 7.77–7.84 (2H, m, Ph). ^{13}C NMR ($CDCl_3$): δ 16.49, 18.37 (2 × s, Me), 25.62 (s, C(4)), 63.56 (s, C(3)), 111.28 (t, *J*(CP) 2 Hz, C(2)), 127.04–134.11 (m, Ph and C(6,7)), 140.10 (d, *J*(CP) 27.1 Hz, *ipso* C), 141.09 (d, *J*(CP) 22.9 Hz, *ipso* C), 194.53 (t, *J*(CP) 7.6 Hz, CO), 196.03 (s, CO), 196.18 (s, CO), 197.34 (s, CO), 199.48 (s, CO), 199.64 (s, CO), 200.13 (s, CO), 200.654 (s, CO), 201.49 (s, CO), 201.71 (s, CO), 201.92 (s, CO), 202.12 (s, CO), 202.66 (s, CO). FAB MS (*m/z*) 1243, $[M]^+$; loss of 12 CO groups.

A second red band (R_f 0.45) was recrystallised from CH_2Cl_2/MeOH to yield **7** (26 mg, 14%), $[M-CO]^+$ 1149. $C_{41}H_{27}O_{12}P_2Ru_4$ requires M, 1177). IR (cyclohexane): ν(CO) 2079s, 2062vs, 2045vw, 2037w, 2023vs, 2018s, 2000(sh), 1997m, 1975(sh), 1971w, 1965m, 1958w, 1818w cm^{-1}. FAB MS (*m/z*) 1149, [M – CO]; loss of 10 CO groups. A third red band (R_f 0.35) was recrystallised from CH_2Cl_2/MeOH to yield **9** (15 mg, 8%) [3]. Some starting material (R_f 0.5) was also recovered (41 mg, 21%). A brown band (R_f 0.4; 8 mg) has not yet been identified.

5.4. *Reaction between 1 and 1-butene*

A solution of **1** (150 mg, 0.12 mmol) in benzene (15 ml) was added to a Carius tube (40 ml) and 1-butene (1.84 g, 32.9 mmol) was condensed into it. After heating of the mixture at 87°C for 14 d the excess gas was vented and the solvent removed under reduced pressure. Preparative TLC (petroleum ether/acetone 9/1) of the residue separated seventeen bands, of which four were collected. A brown band (R_f 0.55) was crystallized (CH_2Cl_2/petroleum spirit) as brown microcrystalline **6a** (16 mg, 0.013 mmol, 10%), m.p. 139–141°C. (Found: C, 36.73; H, 2.09; M, 1270 (mass spectrometry). $C_{40}H_{30}O_{12}P_2Ru_5 \cdot 0.5CH_2Cl_2$ calcd.: C, 35.87; H, 2.36; M, 1270 (unsolvated).) IR (cyclohexane): ν(CO) 2078m, 2047s, 2029s, 2023(sh), 2013s, 1997m, 1989(sh), 1979m, 1972w, 1951vw cm^{-1}. ^1H NMR (C_6D_6): δ 8.1–6.4 (15H, m, Ph), 6.21 (1H, dt, *J*(HH) 15.6 6.2 Hz, =CH), 6.00 (1H, m, =CH), 5.40 (1H, d, *J*(HH) 15.7 Hz, =CH),5.27 (2H, s, CH_2Cl_2), 1.90 (2H, m, CH_2), 1.75 (2H, m, CH_2), 1.37 (2H, m, CH_2), 1.00 (2H, m, CH_2), 0.96 (3H, t, *J*(HH) 7.6 Hz, CH_3), 0.73 (3H, t, $J = 7.2$ Hz, CH_3). FAB MS: 1270, $[M]^+$; loss of 10 CO groups. This compound decomposed readily in solution. The following major orange band (R_f 0.45) was crystallized quickly (CH_2Cl_2/pentane) to give orange plates of **6b** (31 mg, 0.024 mmol, 20%), m.p. 170°C (decomposes). (Found: C, 37.58; H, 2.36; M, 1270 (mass spectrometry). $C_{40}H_{30}O_{12}P_2Ru_5$ calcd.: C, 37.80; H, 2.36; M, 1270.) IR (cyclohexane): ν(CO) 2069m, 2037s, 2022(sh), 2016s, 2008(sh), 1994(sh), 1982vw, 1958w cm^{-1}. ^1H NMR (C_6D_6): δ 7.9–6.7 (15H, m, Ph), 5.44 (2H, dt, *J*(HH) 15.9, 6.1 Hz, =CH), 4.99 (1H, d, *J*(HH) 16.0 Hz, =CH), 1.81 (2H, m, CH_2), 1.51 (2H, m, CH_2), 1.38 (1H, m, CH_2), 1.23 (1H, m, CH_2), 0.87 (3H, t, *J*(HH) 7.4 Hz, CH_3), 0.70 (3H, t, *J*(HH) 7.0 Hz, CH_3). FAB MS: 1270, $[M]^+$; loss of nine CO groups, intensities similar to **6a**. Within 30 min of being placed in solution, isomer-pure **6b** was partially converted to **6a** and, conversely, pure **6a** to **6b**. The next minor band removed (R_f 0.38, brown) was fractionally crystallised (CH_2Cl_2/cyclohexane) to give an orange powder which was formulated as $Ru_5(CO)_{12}(PPh)(PPh_2)\{C_2(C_4H_8)_3\}$. IR (cyclohexane): ν(CO) 2070w, 2037s, 2023(sh), 2010vs, 1978w, 1972w cm^{-1}; FAB MS: 1382, $[M]^+$, loss of 11 CO groups. The last band removed (R_f 0.25, red) was given the formulation $Ru_5(CO)_{11}(dppa^*)(C_4H_8)$ on the basis of spectroscopic data: IR (cyclohexane): ν(CO) 2081w, 2053m, 2037(sh), 2025vs, 2013s, 2000(sh), 1992m, 1982(sh), 1967w, 1950w, 1768vw cm^{-1}; FAB MS: 1265, $[M]^+$, loss of eight CO groups. Insufficient amounts of these last two products were obtained to allow full characterization.

5.5. *Synthesis of $Ru_5(\mu_4\text{-}PPh)(\mu\text{-}PPh_2)(\mu\text{-}CO)(CO)_{10}\{\eta^5\text{-}C_5H_3Me\text{-}1\text{-}(CH{=}CH_2)\text{-}3\}$ (8)*

5.5.1. *Reaction of 1 with ethene*

Ethene was bubbled through a solution of **1** (100 mg, 0.079 mmol) in cyclohexane (50 ml) at slow reflux (oil bath 105°C). After 48 h the mixture was cooled and the solvent removed under reduced pressure. Preparative TLC (petroleum ether/CH_2Cl_2 7/1) of the reaction product separated nine bands from a large baseline; five were collected. A trace green band (R_f 0.51) was identified (IR, FAB MS) as $Ru_5(\mu\text{-}H)(\mu_4\text{-}PPh)\{\mu_4\text{-}\eta^4\text{-}CCPh(C_6H_4)\}(\mu_3\text{-}PPh)(CO)_{10}$ [18b]. The next orange band was further chromatographed (TLC: petroleum ether/acetone 9/1) to give two bands, a brown band (R_f 0.44) identified (IR, FAB MS) as **4a** and an orange band (R_f 0.33) which contained **4b**. Two other products obtained from the original separation (brown bands at R_f 0.43, 0.40 respectively) have the same nominal formulation, *viz* $Ru_5(CO)_{12n}(dppa^*)(C_2H_4)_n$ (FAB MS: 1237, $[M]^+$). The last brown band collected (R_f 0.29) was repurified (preparative TLC: petroleum ether/CH_2Cl_2/acetone 8/2/1) to give a major brown band (R_f 0.55), this in turn was fractionally crystallized (CH_2Cl_2/petroleum ether) to give brown crystals of **8** (9 mg, 0.007 mmol, 9%), m.p. 110–115°C. (Found: C, 39.78; H, 3.08; $[M+2H]^+$, 1214 (mass spectrometry). $C_{37}H_{24}O_{11}P_2Ru_5 \cdot C_6H_{14}$ calcd.: C, 39.75; H, 2.93%; M, 1212 (unsolvated).) IR (cyclohexane): ν(CO) 2060m, 2029vs, 2021(sh), 2012m, 1997(sh), 1987m, 1972w, 1967(sh), 1779vw cm^{-1}. FAB MS: 1214, $[M+2H]^+$; loss of 11 CO groups.

5.5.2. *Conversion of 4a to 8*

A solution of **4a** (12 mg, 0.01 mmol) was dissolved in cyclohexane (30 ml) and heated (oil bath, 98°C, 24 h) with ethene bubbling through the solution. After cooling the solvent was removed under reduced pressure and the residue purified by TLC (petroleum ether/CH_2Cl_2/acetone 8/2/1). Of the seven bands which separated from the base-line only three were collected and identified (IR, spot TLC) as: (1) R_f 0.69, brown, **4a** (0.5 mg, 0.0004 mmol, 4%); (2) R_f 0.63, orange, **4b** (2.0 mg, 0.0016 mmol, 16%); (3) R_f 0.4, brown, **8** (2.4 mg, 0.02 mmol, 19%), also identified by FAB MS.

6. Crystallography

Unique data sets for **4a**, **5b** and **8** were measured at *ca.* 295 K within the specified $2\theta_{max}$ limits using Enraf-Nonius CAD4 diffractometers ($2\theta/\theta$ scan mode; monochromatic Mo-Kα radiation, λ 0.7107_3 Å). N independent reflections were obtained, N_o with $I > 3\sigma(I)$ being considered 'observed' and used in the full matrix least squares refinement after absorption correction. For all, anisotropic thermal parameters were refined for the non-hydrogen atoms (except for C(6) and C(6′) in **4a**); $(x, y, z, U_{iso})_H$ were included constrained at estimated values. In **4a**, the position of the C(6) atom was found to be disordered over two positions and hence both sites were refined with fractional site occupancies summing to unity; the major occupancy was 0.557(2) for the C(6) atom as illustrated in Fig. 1(a). Conventional residuals R, R' on $|F|$ are quoted, refinement of **4a** being continued with a weighting scheme of the form $w = k/[\sigma^2(F) + |g|F^2]$, with $k = 2.46$ and $g = 0.001$ at convergence. For **5b** and **8**, statistical weights derivative of $\sigma^2(I) = \sigma^2(I_{diff}) + 0.0004\sigma^4(I_{diff})$ were used. Computation used the SHELX programs [19,20] (**4a**) and XTAL 2.6 program system implemented by Hall and Stewart [21] (**5b** and **8**); neutral atom complex scattering factors were employed [22].

The crystallographic numbering schemes are given in Fig. 1 (drawn with the ORTEP program [23]) and selected interatomic parameters are listed in Tables 1 and 2. Tables of thermal parameters, H-atom parameters, all bond distances and angles, and tables of observed and calculated structure factors are available from the authors.

Acknowledgements

We thank the Australian Research Council for financial support and Johnson Matthey Technology Centre for a generous loan of $RuCl_3 \cdot nH_2O$. MJL was the holder of a Commonwealth Post-Graduate Research Award.

References

1 Part 82: M. I. Bruce, P. A. Humphrey, E. Horn, B. W. Skelton, E. R. T. Tiekink and A. H. White, *J. Organomet. Chem., 429* (1992) 207.

2 C. J. Adams, M. I. Bruce, M. J. Liddell, B. W. Skelton and A. H. White, *Organometallics, 11* (1992) 1182.

3 Part 84: C. J. Adams, M. I. Bruce, B. W. Skelton and A. H. White, *J. Organomet. Chem., 445* (1993) 199.

4 M. I. Bruce, M. R. Snow, E. R. T. Tiekink and M. L. Williams, *J. Chem. Soc., Chem. Commun.,* (1986) 701.

5 C. J. Adams, M. I. Bruce, B. W. Skelton and A. H. White, *J. Organomet. Chem., 423* (1992) 97.

6 C. J. Adams, M. I. Bruce, B. W. Skelton and A. H. White, *J. Chem. Soc., Chem. Commun.,* (1992) 26.

7 M. I. Bruce, B. W. Skelton, A. H. White and M. L. Williams, *J. Organomet. Chem., 369* (1989) 393.

8 S. A. R. Knox and M. J. Morris, *J. Chem. Soc., Dalton Trans.,* (1987) 2087.

9 A. G. Cowie, B. F. G. Johnson, J. Lewis, J. N. Nicholls, P. R. Raithby and A. G. Swanson, *J. Chem. Soc., Chem. Commun.,* (1984) 637.

10 (a) M. O. Albers, D. J. Robinson and E. Singleton, *Coord. Chem. Rev., 79* (1987) 1; (b) L. R. Nevinger, J. B. Keister, C. H. Lake and M. R. Churchill, *Organometallics, 11* (1992) 1819.

11 A. J. Deeming, S. Hasso and M. Underhill, *J. Chem. Soc., Dalton Trans.,* (1975) 1614; J. B. Keister and J. R. Shapley, *J. Organomet. Chem., 85* (1975) C29.

12 (a) R. Ros, R. Roulet and A. Scrivanti, *J. Organomet. Chem., 303* (1986) 273; (b) J. R. Shapley and M. Tachikawa, *J. Organomet. Chem., 124* (1977) C19; (c) Y. J. Chen, C. B. Knobler and H. D. Kaesz, *Polyhedron, 7* (1988) 1891.

13 P. F. Jackson, B. F. G. Johnson, J. Lewis, P. R. Raithby, G. J. Will, M. McPartlin and W. J. H. Nelson, *J. Chem. Soc., Chem. Commun.,* (1980) 1190.

14 F. Garin and G. Maire, *J. Mol. Cat., 48* (1988) 99.

15 (a) R. B. Anderson, *The Fischer–Tropsch Synthesis,* Academic, New York, 1984; (b) B. D. Dombek, *Adv. Catal., 32* (1983) 325; (c) C. K. Roofer-DePoorter, *Chem. Rev., 81* (1981) 447.

16 D. R. Neithamer, R. E. LaPointe, R. A. Wheeler, D. S. Richeson, G. D. van Duyne and P. T. Wolczanski, *J. Am. Chem. Soc., 111* (1989) 9056.

17 C. J. Adams and M. I. Bruce, unpublished results.
18 (a) M. I. Bruce, M. L. Williams, J. M. Patrick and A. H. White, *J. Chem. Soc., Dalton Trans.*, (1985) 1229; (b) M. I. Bruce, M. J. Liddell and E. R. T. Tiekink, *J. Organomet. Chem.*, *391* (1990) 81.
19 G. M. Sheldrick, *SHELX76, Programme for crystal structure determination*, University of Cambridge, 1976.
20 G. M. Sheldrick, *SHELXS86, Programme for the automatic solution of crystal structures*, University of Göttingen, 1978.
21 S. R. Hall and J. M. Stewart (eds.), *XTAL Users' Manual, Version 2.6*, Universities of Western Australia and Maryland, 1989.
22 J. A. Ibers and W. C. Hamilton, *International Tables for Crystallography*, Vol. 4, Kynoch Press, Birmingham, 1974, pp. 99, 149.
23 C. K. Johnson, *ORTEP-II, Report ORNL-5138*, Oak Ridge National Laboratory, Tennessee, 1976.